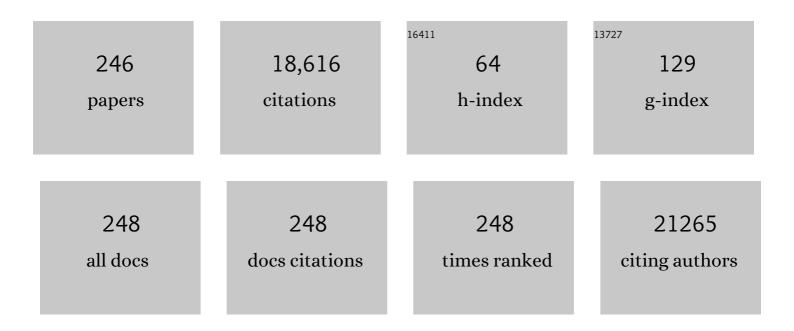
## Cheng-Te Lin

List of Publications by Year in descending order

Source: https://exaly.com/author-pdf/5789327/publications.pdf Version: 2024-02-01



#	Article	IF	CITATIONS
1	Synthesis of Largeâ€Area MoS <sub>2</sub> Atomic Layers with Chemical Vapor Deposition. Advanced Materials, 2012, 24, 2320-2325.	11.1	2,956
2	Element Replacement Approach by Reaction with Lewis Acidic Molten Salts to Synthesize Nanolaminated MAX Phases and MXenes. Journal of the American Chemical Society, 2019, 141, 4730-4737.	6.6	811
3	Highly Efficient Electrocatalytic Hydrogen Production by MoS <i><sub>x</sub></i> Grown on Grapheneâ€Protected 3D Ni Foams. Advanced Materials, 2013, 25, 756-760.	11.1	693
4	Synthesis and Transfer of Single-Layer Transition Metal Disulfides on Diverse Surfaces. Nano Letters, 2013, 13, 1852-1857.	4.5	612
5	Graphene-modified LiFePO4 cathode for lithium ion battery beyond theoretical capacity. Nature Communications, 2013, 4, 1687.	5.8	481
6	A Twoâ€Dimensional Zirconium Carbide by Selective Etching of Al <sub>3</sub> C <sub>3</sub> from Nanolaminated Zr <sub>3</sub> Al <sub>3</sub> C <sub>5</sub> . Angewandte Chemie - International Edition, 2016, 55, 5008-5013.	7.2	425
7	Synthesis and Electrochemical Properties of Two-Dimensional Hafnium Carbide. ACS Nano, 2017, 11, 3841-3850.	7.3	370
8	Volumetric solar heating of nanofluids for direct vapor generation. Nano Energy, 2015, 17, 290-301.	8.2	350
9	Largeâ€Area Ultrathin Graphene Films by Singleâ€Step Marangoni Selfâ€Assembly for Highly Sensitive Strain Sensing Application. Advanced Functional Materials, 2016, 26, 1322-1329.	7.8	326
10	Graphene/MoS <sub>2</sub> Heterostructures for Ultrasensitive Detection of DNA Hybridisation. Advanced Materials, 2014, 26, 4838-4844.	11.1	290
11	Role of the surface effect on the structural, electronic and mechanical properties of the carbide MXenes. Europhysics Letters, 2015, 111, 26007.	0.7	262
12	Enhanced thermal properties of poly(vinylidene fluoride) composites with ultrathin nanosheets of MXene. RSC Advances, 2017, 7, 20494-20501.	1.7	242
13	Rational Design of Flexible Two-Dimensional MXenes with Multiple Functionalities. Chemical Reviews, 2019, 119, 11980-12031.	23.0	242
14	Opening an Electrical Band Gap of Bilayer Graphene with Molecular Doping. ACS Nano, 2011, 5, 7517-7524.	7.3	222
15	Metal-Level Thermally Conductive yet Soft Graphene Thermal Interface Materials. ACS Nano, 2019, 13, 11561-11571.	7.3	214
16	A self-powered high-performance graphene/silicon ultraviolet photodetector with ultra-shallow junction: breaking the limit of silicon?. Npj 2D Materials and Applications, 2017, 1, .	3.9	211
17	Promising electron mobility and high thermal conductivity in Sc <sub>2</sub> CT <sub>2</sub> (T = F,) Tj ETQq1	1 0.784314 2.8	4 rgBT /Ove 205
18	Layer-by-Layer Graphene/TCNQ Stacked Films as Conducting Anodes for Organic Solar Cells. ACS Nano, 2012 6, 5031-5039	7.3	199

2012, 6, 5031-5039.

#	Article	IF	CITATIONS
19	Thermal conductivity enhancement of phase change materials with 3D porous diamond foam for thermal energy storage. Applied Energy, 2019, 233-234, 208-219.	5.1	194
20	Ultrahigh-Aspect-Ratio Boron Nitride Nanosheets Leading to Superhigh In-Plane Thermal Conductivity of Foldable Heat Spreader. ACS Nano, 2021, 15, 6489-6498.	7.3	191
21	Label-free detection of DNA hybridization using transistors based on CVD grown graphene. Biosensors and Bioelectronics, 2013, 41, 103-109.	5.3	185
22	New Deformation-Induced Nanostructure in Silicon. Nano Letters, 2018, 18, 4611-4617.	4.5	182
23	The thermal and electrical properties of the promising semiconductor MXene Hf2CO2. Scientific Reports, 2016, 6, 27971.	1.6	178
24	Enhanced thermal conductivity for polyimide composites with a three-dimensional silicon carbide nanowire@graphene sheets filler. Journal of Materials Chemistry A, 2015, 3, 4884-4891.	5.2	173
25	Controlled porous structures of graphene aerogels and their effect on supercapacitor performance. Nanoscale, 2015, 7, 4386-4393.	2.8	163
26	Enhanced thermal conductivity of polyurethane composites via engineering small/large sizes interconnected boron nitride nanosheets. Composites Science and Technology, 2019, 170, 93-100.	3.8	160
27	Constructing a "pea-pod-like―alumina-graphene binary architecture for enhancing thermal conductivity of epoxy composite. Chemical Engineering Journal, 2020, 381, 122690.	6.6	157
28	In situ formation of a cellular graphene framework in thermoplastic composites leading to superior thermal conductivity. Journal of Materials Chemistry A, 2017, 5, 6164-6169.	5.2	149
29	An ultrathin high-performance heat spreader fabricated with hydroxylated boron nitride nanosheets. 2D Materials, 2017, 4, 025047.	2.0	145
30	Highly thermal conductive and electrical insulating polymer composites with boron nitride. Composites Part B: Engineering, 2020, 184, 107746.	5.9	142
31	Intrinsic Structural, Electrical, Thermal, and Mechanical Properties of the Promising Conductor Mo <sub>2</sub> C MXene. Journal of Physical Chemistry C, 2016, 120, 15082-15088.	1.5	139
32	A Paper-Like Inorganic Thermal Interface Material Composed of Hierarchically Structured Graphene/Silicon Carbide Nanorods. ACS Nano, 2019, 13, 1547-1554.	7.3	131
33	Defects regulating of graphene ink for electrochemical determination of ascorbic acid, dopamine and uric acid. Talanta, 2018, 180, 248-253.	2.9	124
34	3D Shapeable, Superior Electrically Conductive Cellulose Nanofibers/Ti <sub>3</sub> C <sub>2</sub> T <sub>x</sub> MXene Aerogels/Epoxy Nanocomposites for Promising EMI Shielding. Research, 2020, 2020, 4093732.	2.8	124
35	Extreme sensitivity of graphene photoconductivity to environmental gases. Nature Communications, 2012, 3, 1228.	5.8	120
36	Highly thermal conductive polymer composites via constructing micro-phragmites communis structured carbon fibers. Chemical Engineering Journal, 2019, 375, 121921.	6.6	115

#	Article	IF	CITATIONS
37	Labelâ€Free Electrical Detection of DNA Hybridization on Graphene using Hall Effect Measurements: Revisiting the Sensing Mechanism. Advanced Functional Materials, 2013, 23, 2301-2307.	7.8	114
38	Highly stable and regenerative graphene–diamond hybrid electrochemical biosensor for fouling target dopamine detection. Biosensors and Bioelectronics, 2018, 111, 117-123.	5.3	112
39	A Broadband Fluorographene Photodetector. Advanced Materials, 2017, 29, 1700463.	11.1	110
40	Graphene woven fabric-reinforced polyimide films with enhanced and anisotropic thermal conductivity. Composites Part A: Applied Science and Manufacturing, 2016, 87, 290-296.	3.8	108
41	Multiscale Structural Modulation of Anisotropic Graphene Framework for Polymer Composites Achieving Highly Efficient Thermal Energy Management. Advanced Science, 2021, 8, 2003734.	5.6	108
42	Exceptionally high thermal and electrical conductivity of three-dimensional graphene-foam-based polymer composites. RSC Advances, 2016, 6, 22364-22369.	1.7	105
43	Enhanced thermal conductivity of epoxy composites filled with silicon carbide nanowires. Scientific Reports, 2017, 7, 2606.	1.6	105
44	Graphene foam-embedded epoxy composites with significant thermal conductivity enhancement. Nanoscale, 2019, 11, 17600-17606.	2.8	105
45	Enhanced Thermal Conductivity of Epoxy Composites Filled with 2D Transition Metal Carbides (MXenes) with Ultralow Loading. Scientific Reports, 2019, 9, 9135.	1.6	104
46	Self-Assembled Graphene Film as Low Friction Solid Lubricant in Macroscale Contact. ACS Applied Materials & Interfaces, 2017, 9, 21554-21562.	4.0	103
47	Soft and Selfâ€Adhesive Thermal Interface Materials Based on Vertically Aligned, Covalently Bonded Graphene Nanowalls for Efficient Microelectronic Cooling. Advanced Functional Materials, 2021, 31, 2104062.	7.8	95
48	Graphene size-dependent modulation of graphene frameworks contributing to the superior thermal conductivity of epoxy composites. Journal of Materials Chemistry A, 2018, 6, 12091-12097.	5.2	88
49	A flexible hydrophilic-modified graphene microprobe for neural and cardiac recording. Nanomedicine: Nanotechnology, Biology, and Medicine, 2013, 9, 600-604.	1.7	86
50	Infrageneric phylogenetics investigation of Chimonanthus based on electroactive compound profiles. Bioelectrochemistry, 2020, 133, 107455.	2.4	86
51	Flammability, thermal stability and mechanical properties of polyvinyl alcohol nanocomposites reinforced with delaminated Ti <sub>3</sub> C <sub>2</sub> T <sub><i>x</i></sub> (MXene). Polymer Composites, 2020, 41, 210-218.	2.3	84
52	Extremely high thermal conductivity of carbon fiber/epoxy with synergistic effect of MXenes by freeze-drying. Composites Communications, 2020, 19, 134-141.	3.3	81
53	A glassy carbon electrode modified with N-doped carbon dots for improved detection of hydrogen peroxide and paracetamol. Mikrochimica Acta, 2018, 185, 87.	2.5	80
54	Enhanced Electrocatalytic Activity of MoS <sub><i>x</i></sub> on TCNQ-Treated Electrode for Hydrogen Evolution Reaction. ACS Applied Materials & Interfaces, 2014, 6, 17679-17685.	4.0	78

#	Article	IF	CITATIONS
55	High-Thermal-Transport-Channel Construction within Flexible Composites via the Welding of Boron Nitride Nanosheets. ACS Applied Nano Materials, 2019, 2, 360-368.	2.4	78
56	Large-area self-assembled reduced graphene oxide/electrochemically exfoliated graphene hybrid films for transparent electrothermal heaters. Applied Surface Science, 2018, 435, 809-814.	3.1	77
57	Stress induced carbon fiber orientation for enhanced thermal conductivity of epoxy composites. Composites Part B: Engineering, 2021, 208, 108599.	5.9	76
58	Lycoris species identification and infrageneric relationship investigation via graphene enhanced electrochemical fingerprinting of pollen. Sensors and Actuators B: Chemical, 2019, 298, 126836.	4.0	75
59	Tailoring Highly Ordered Graphene Framework in Epoxy for High-Performance Polymer-Based Heat Dissipation Plates. ACS Nano, 2021, 15, 12922-12934.	7.3	75
60	Cotton Candy-Templated Fabrication of Three-Dimensional Ceramic Pathway within Polymer Composite for Enhanced Thermal Conductivity. ACS Applied Materials & amp; Interfaces, 2019, 11, 44700-44707.	4.0	74
61	Growth selectivity of hexagonal-boron nitride layers on Ni with various crystal orientations. RSC Advances, 2012, 2, 111-115.	1.7	72
62	Delaminated Ti3C2Tx (MXene) for electrochemical carbendazim sensing. Materials Letters, 2019, 236, 412-415.	1.3	72
63	Rational design of graphene/polymer composites with excellent electromagnetic interference shielding effectiveness and high thermal conductivity: a mini review. Journal of Materials Science and Technology, 2022, 117, 238-250.	5.6	72
64	An electrochemical method for plant species determination and classification based on fingerprinting petal tissue. Bioelectrochemistry, 2019, 129, 199-205.	2.4	71
65	Highly flexible biodegradable cellulose nanofiber/graphene heat-spreader films with improved mechanical properties and enhanced thermal conductivity. Journal of Materials Chemistry C, 2018, 6, 12739-12745.	2.7	69
66	In Situ High-Pressure X-ray Diffraction and Raman Spectroscopy Study of Ti3C2Tx MXene. Nanoscale Research Letters, 2018, 13, 343.	3.1	67
67	Enhanced electrochemical voltammetric fingerprints for plant taxonomic sensing. Biosensors and Bioelectronics, 2018, 120, 102-107.	5.3	67
68	Development of an electrochemical biosensor for phylogenetic analysis of Amaryllidaceae based on the enhanced electrochemical fingerprint recorded from plant tissue. Biosensors and Bioelectronics, 2020, 159, 112212.	5.3	66
69	A Twoâ€Dimensional Zirconium Carbide by Selective Etching of Al <sub>3</sub> C <sub>3</sub> from Nanolaminated Zr <sub>3</sub> Al <sub>3</sub> C <sub>5</sub> . Angewandte Chemie, 2016, 128, 5092-5097.	1.6	65
70	Macroscale Superlubricity Enabled by Graphene oated Surfaces. Advanced Science, 2020, 7, 1903239.	5.6	64
71	A novel modification to boron-doped diamond electrode for enhanced, selective detection of dopamine in human serum. Carbon, 2021, 171, 16-28.	5.4	64
72	Graphene-based electrochemical sensors for antibiotic detection in water, food and soil: A scientometric analysis in CiteSpace (2011–2021). Chemosphere, 2022, 297, 134127.	4.2	62

#	Article	IF	CITATIONS
73	Long-term stability of Au nanoparticle-anchored porous boron-doped diamond hybrid electrode for enhanced dopamine detection. Electrochimica Acta, 2018, 271, 84-91.	2.6	61
74	Hall effect biosensors with ultraclean graphene film for improved sensitivity of label-free DNA detection. Biosensors and Bioelectronics, 2018, 99, 85-91.	5.3	60
75	Direct formation of wafer-scale single-layer graphene films on the rough surface substrate by PECVD. Carbon, 2018, 129, 456-461.	5.4	60
76	Thermal conductivity and mechanical properties of flake graphite/copper composite with a boron carbide-boron nano-layer on graphite surface. Composites Part A: Applied Science and Manufacturing, 2018, 106, 42-51.	3.8	58
77	Effective thermal transport highway construction within dielectric polymer composites <i>via</i> a vacuum-assisted infiltration method. Journal of Materials Chemistry C, 2018, 6, 6494-6501.	2.7	57
78	Flexible transparent electrodes made of electrochemically exfoliated graphene sheets from low-cost graphite pieces. Displays, 2013, 34, 315-319.	2.0	56
79	Carbon nanotube-Cu foam hybrid reinforcements in composite phase change materials with enhanced thermal conductivity. Materials and Design, 2019, 172, 107709.	3.3	56
80	Enhanced thermal conductivity for poly(vinylidene fluoride) composites with nano-carbon fillers. RSC Advances, 2016, 6, 68357-68362.	1.7	55
81	High quality graphene films with a clean surface prepared by an UV/ozone assisted transfer process. Journal of Materials Chemistry C, 2017, 5, 1880-1884.	2.7	54
82	Boron nitride nanosheet nanofluids for enhanced thermal conductivity. Nanoscale, 2018, 10, 13004-13010.	2.8	54
83	Lightweight thermal interface materials based on hierarchically structured graphene paper with superior through-plane thermal conductivity. Chemical Engineering Journal, 2021, 419, 129609.	6.6	54
84	Enhanced Electromagnetic Shielding and Thermal Conductive Properties of Polyolefin Composites with a Ti <sub>3</sub> C <sub>2</sub> T <sub><i>x</i></sub> MXene/Graphene Framework Connected by a Hydrogen-Bonded Interface. ACS Nano, 2022, 16, 9254-9266.	7.3	54
85	In situ growth of metal nanoparticles on boron nitride nanosheets as highly efficient catalysts. Journal of Materials Chemistry A, 2016, 4, 19107-19115.	5.2	52
86	Tuning the Electrical Conductivity of Ti <sub>2</sub> CO <sub>2</sub> MXene by Varying the Layer Thickness and Applying Strains. Journal of Physical Chemistry C, 2019, 123, 6802-6811.	1.5	49
87	Construction of 3D interconnected diamond networks in Al-matrix composite for high-efficiency thermal management. Chemical Engineering Journal, 2020, 380, 122551.	6.6	49
88	Electronic and Transport Properties of Ti <sub>2</sub> CO <sub>2</sub> MXene Nanoribbons. Journal of Physical Chemistry C, 2016, 120, 17143-17152.	1.5	46
89	Combining Alumina Particles with Three-Dimensional Alumina Foam for High Thermally Conductive Epoxy Composites. ACS Applied Polymer Materials, 2021, 3, 216-225.	2.0	45
90	Continuous diamond-carbon nanotube foams as rapid heat conduction channels in composite phase change materials based on the stable hierarchical structure. Composites Part B: Engineering, 2020, 200, 108293.	5.9	44

#	Article	IF	CITATIONS
91	Electrochemical antioxidant screening based on a chitosan hydrogel. Bioelectrochemistry, 2018, 121, 7-10.	2.4	43
92	Electrochemical Sex Determination of Dioecious Plants Using Polydopamine-Functionalized Graphene Sheets. Frontiers in Chemistry, 2020, 8, 92.	1.8	43
93	A solid-state electrochemical sensing platform based on a supramolecular hydrogel. Sensors and Actuators B: Chemical, 2018, 262, 326-333.	4.0	41
94	Enhanced thermal conductivity of epoxy composites filled with tetrapod-shaped ZnO. RSC Advances, 2018, 8, 12337-12343.	1.7	41
95	Rapid growth of single-layer graphene on the insulating substrates by thermal CVD. Applied Surface Science, 2015, 346, 41-45.	3.1	40
96	Sensitivity enhancement of potassium ion (K+) detection based on graphene field-effect transistors with surface plasma pretreatment. Sensors and Actuators B: Chemical, 2019, 285, 333-340.	4.0	40
97	Efficient Thermal Transport Highway Construction Within Epoxy Matrix via Hybrid Carbon Fibers and Alumina Particles. ACS Omega, 2020, 5, 1170-1177.	1.6	39
98	Highly thermally conductive polymer composites with barnacle-like nano-crystalline Diamond@Silicon carbide hybrid architecture. Composites Part B: Engineering, 2020, 198, 108167.	5.9	39
99	Electrochemical Fingerprint Biosensor for Natural Indigo Dye Yielding Plants Analysis. Biosensors, 2021, 11, 155.	2.3	39
100	Electrical Probing of Submicroliter Liquid Using Graphene Strip Transistors Built on a Nanopipette. Small, 2012, 8, 43-46.	5.2	38
101	High-Quality Monolithic Graphene Films via Laterally Stitched Growth and Structural Repair of Isolated Flakes for Transparent Electronics. Chemistry of Materials, 2017, 29, 7808-7815.	3.2	38
102	Highly Conductive 3D Segregated Graphene Architecture in Polypropylene Composite with Efficient EMI Shielding. Polymers, 2017, 9, 662.	2.0	38
103	Highly flexible few-layer Ti <sub>3</sub> C <sub>2</sub> MXene/cellulose nanofiber heat-spreader films with enhanced thermal conductivity. New Journal of Chemistry, 2020, 44, 7186-7193.	1.4	38
104	<i>In situ</i> TEM observation of rebonding on fractured silicon carbide. Nanoscale, 2018, 10, 6261-6269.	2.8	37
105	Graphene-Based Thermal Interface Materials: An Application-Oriented Perspective on Architecture Design. Polymers, 2018, 10, 1201.	2.0	37
106	Crystal structure and encapsulation dynamics of ice II-structured neon hydrate. Proceedings of the National Academy of Sciences of the United States of America, 2014, 111, 10456-10461.	3.3	36
107	Square wave voltammetric quantitative determination of flavonoid luteolin in peanut hulls and Perilla based on Au NPs loaded boron nitride nanosheets. Journal of Electroanalytical Chemistry, 2018, 817, 128-133.	1.9	35
108	Coal ash fusion properties from molecular dynamics simulation: the role of calcium oxide. Fuel, 2018, 216, 760-767.	3.4	35

#	Article	IF	CITATIONS
109	Negative differential resistance and rectifying performance induced by doped graphene nanoribbons p – n device. Physics Letters, Section A: General, Atomic and Solid State Physics, 2016, 380, 1049-1055.	0.9	34
110	Graphene Structure in Carbon Nanocones and Nanodiscs. Langmuir, 2007, 23, 12806-12810.	1.6	33
111	Anisotropic electrical conduction of vertically-aligned single-walled carbon nanotube films. Carbon, 2011, 49, 1446-1452.	5.4	33
112	Effect of different sizes of graphene on thermal transport performance of graphene paper. Composites Communications, 2017, 5, 46-53.	3.3	32
113	A novel approach to fabricating a nanotwinned surface on a ternary nickel alloy. Materials and Design, 2016, 106, 313-320.	3.3	31
114	Macroporous diamond foam: A novel design of 3D interconnected heat conduction network for thermal management. Materials and Design, 2018, 156, 32-41.	3.3	31
115	An Ultrasensitive Contact Lens Sensor Based On Selfâ€Assembly Graphene For Continuous Intraocular Pressure Monitoring. Advanced Functional Materials, 2021, 31, 2010991.	7.8	31
116	Synergistic effect of carbon fiber and graphite on reducing thermal resistance of thermal interface materials. Composites Science and Technology, 2021, 212, 108883.	3.8	31
117	Exploring the potential of exfoliated ternary ultrathin Ti <sub>4</sub> AlN <sub>3</sub> nanosheets for fabricating hybrid patterned polymer brushes. RSC Advances, 2015, 5, 70339-70344.	1.7	30
118	In Situ TEM Study of Interaction between Dislocations and a Single Nanotwin under Nanoindentation. ACS Applied Materials & Interfaces, 2017, 9, 29451-29456.	4.0	30
119	Two-dimensional semiconducting Lu <sub>2</sub> CT <sub>2</sub> (T = F, OH) MXene with low work function and high carrier mobility. Nanoscale, 2020, 12, 3795-3802.	2.8	30
120	Efficient Heat Dissipation of Photonic Crystal Microcavity by Monolayer Graphene. ACS Nano, 2013, 7, 10818-10824.	7.3	29
121	Anisotropic thermal conductive properties of cigarette filter-templated graphene/epoxy composites. RSC Advances, 2018, 8, 1065-1070.	1.7	29
122	All-carbon devices based on sp2-on-sp3 configuration. APL Materials, 2019, 7, .	2.2	29
123	Improving thermal conductivity of poly(vinyl alcohol) composites by using functionalized nanodiamond. Composites Communications, 2021, 23, 100596.	3.3	29
124	Crystallization induced realignment of carbon fibers in a phase change material to achieve exceptional thermal transportation properties. Journal of Materials Chemistry A, 2022, 10, 593-601.	5.2	29
125	Solid-Phase Coalescence of Electrochemically Exfoliated Graphene Flakes into a Continuous Film on Copper. Chemistry of Materials, 2016, 28, 3360-3366.	3.2	28
126	High-performance non-enzymatic glucose sensor based on Ni/Cu/boron-doped diamond electrode. Journal of Electroanalytical Chemistry, 2019, 841, 135-141.	1.9	28

#	Article	IF	CITATIONS
127	Viscosity temperature properties from molecular dynamics simulation: The role of calcium oxide, sodium oxide and ferrous oxide. Fuel, 2019, 237, 163-169.	3.4	28
128	Ultrasensitive micro/nanocrack-based graphene nanowall strain sensors derived from the substrate's Poisson's ratio effect. Journal of Materials Chemistry A, 2020, 8, 10310-10317.	5.2	28
129	Epoxy composites filled with one-dimensional SiC nanowires–two-dimensional graphene nanoplatelets hybrid nanofillers. RSC Advances, 2014, 4, 59409-59417.	1.7	26
130	New insight into the helium-induced damage in MAX phase Ti3AlC2 by first-principles studies. Journal of Chemical Physics, 2015, 143, 114707.	1.2	26
131	A Diamond Temperature Sensor Based on the Energy Level Shift of Nitrogen-Vacancy Color Centers. Nanomaterials, 2019, 9, 1576.	1.9	26
132	First-principles study of the electronic, optical and transport of few-layer semiconducting MXene. Computational Materials Science, 2019, 168, 137-143.	1.4	26
133	Hierarchical Co3O4@NiMoO4 core-shell nanowires for chemiresistive sensing of xylene vapor. Mikrochimica Acta, 2019, 186, 222.	2.5	26
134	Enhanced thermal conductivity of epoxy composites with coreâ€shell SiC@SiO <sub>2</sub> nanowires. High Voltage, 2017, 2, 154-160.	2.7	25
135	First-principles study on the electrical and thermal properties of the semiconducting Sc <sub>3</sub> (CN)F <sub>2</sub> MXene. RSC Advances, 2018, 8, 22452-22459.	1.7	24
136	Quasi two-dimensional carbon nanobelts synthesized using a template method. Carbon, 2008, 46, 741-746.	5.4	23
137	Tailor Made Mie Scattering Color Filters Made by Size-Tunable Titanium Dioxide Particles. Journal of Physical Chemistry C, 2008, 112, 2697-2702.	1.5	22
138	Tuning the photoluminescence of large Ti3C2Tx MXene flakes. Ceramics International, 2019, 45, 11468-11474.	2.3	22
139	Continuous fabrication platform for highly aligned polymer films. Technology, 2014, 02, 189-199.	1.4	21
140	Electronic structures and mechanical properties of Al(111)/ZrB <sub>2</sub> (0001) heterojunctions from first-principles calculation. Molecular Physics, 2015, 113, 1794-1801.	0.8	21
141	Active-powering pressure-sensing fabric devices. Journal of Materials Chemistry A, 2020, 8, 358-368.	5.2	21
142	A scalable polymer-free method for transferring graphene onto arbitrary surfaces. Carbon, 2020, 161, 479-485.	5.4	21
143	Label-Free Electrochemical Detection of Vanillin through Low-Defect Graphene Electrodes Modified with Au Nanoparticles. Materials, 2018, 11, 489.	1.3	20
144	Electrochemical Voltammogram Recording for Identifying Varieties of Ornamental Plants. Micromachines, 2020, 11, 967.	1.4	20

#	Article	IF	CITATIONS
145	Robust composite film with high thermal conductivity and excellent mechanical properties by constructing a long-range ordered sandwich structure. Journal of Materials Chemistry A, 2022, 10, 9922-9931.	5.2	20
146	Controllable formation of periodic wrinkles in Marangoni-driven self-assembled graphene film for sensitive strain detection. Science China Materials, 2020, 63, 1983-1992.	3.5	19
147	Microwave Irradiationâ€Assisted Exfoliation of Boron Nitride Nanosheets: A Platform for Loading High Density of Nanoparticles. ChemistrySelect, 2016, 1, 1799-1803.	0.7	18
148	Ash Fusion Properties from Molecular Dynamics Simulation: Role of the Ratio of Silicon and Aluminum. Energy & Fuels, 2016, 30, 2407-2413.	2.5	18
149	Chemical vapor deposition growth of scalable monolayer polycrystalline graphene films with millimeter-sized domains. Materials Letters, 2018, 215, 259-262.	1.3	18
150	Effects of Different Surface Functionalization and Doping on the Electronic Transport Properties of M <sub>2</sub> CT <i><sub>x</sub></i> –M <sub>2</sub> CO <sub>2</sub> Heterojunction Devices. Journal of Physical Chemistry C, 2018, 122, 14908-14917.	1.5	18
151	Single-Step Formation of Ni Nanoparticle-Modified Graphene–Diamond Hybrid Electrodes for Electrochemical Glucose Detection. Sensors, 2019, 19, 2979.	2.1	18
152	Structural, mechanical and electronic properties of two-dimensional chlorine-terminated transition metal carbides and nitrides. Journal of Physics Condensed Matter, 2020, 32, 135302.	0.7	18
153	Theoretical investigations on helium trapping in the Zr/Ti 2 AlC interface. Surface and Coatings Technology, 2017, 322, 19-24.	2.2	17
154	Highly Sensitive and Selective Potassium Ion Detection Based on Graphene Hall Effect Biosensors. Materials, 2018, 11, 399.	1.3	17
155	Non-Enzymatic Glucose Sensor Based on Hierarchical Au/Ni/Boron-Doped Diamond Heterostructure Electrode for Improving Performances. Journal of the Electrochemical Society, 2019, 166, B373-B380.	1.3	17
156	Intertwined Carbon Nanotubes and Ag Nanowires Constructed by Simple Solution Blending as Sensitive and Stable Chloramphenicol Sensors. Sensors, 2021, 21, 1220.	2.1	17
157	Surface Modification Using Polydopamine-Coated Liquid Metal Nanocapsules for Improving Performance of Graphene Paper-Based Thermal Interface Materials. Nanomaterials, 2021, 11, 1236.	1.9	17
158	Chloroformâ€Assisted Rapid Growth of Vertical Graphene Array and Its Application in Thermal Interface Materials. Advanced Science, 2022, 9, e2200737.	5.6	17
159	Relationship between graphene and pedosphere: A scientometric analysis. Chemosphere, 2022, 300, 134599.	4.2	17
160	Enhanced thermal conductivity for polydimethylsiloxane composites with core-shell CFs@SiC filler. Composites Communications, 2022, 33, 101209.	3.3	17
161	High Oxidation Resistance of CVD Graphene-Reinforced Copper Matrix Composites. Nanomaterials, 2019, 9, 498.	1.9	16
162	Thermal and corrosion behavior of Ti3C2/Copper composites. Composites Communications, 2020, 22, 100498.	3.3	16

#	Article	IF	CITATIONS
163	Rational design of high-performance thermal interface materials based on gold-nanocap-modified vertically aligned graphene architecture. Composites Communications, 2021, 24, 100621.	3.3	16
164	A mini review: application of graphene paper in thermal interface materials. New Carbon Materials, 2021, 36, 930-938.	2.9	16
165	Constructing Tanghulu-like Diamond@Silicon carbide nanowires for enhanced thermal conductivity of polymer composite. Composites Communications, 2022, 29, 101008.	3.3	16
166	Mobility Enhancement in Carbon Nanotube Transistors by Screening Charge Impurity with Silica Nanoparticles. Journal of Physical Chemistry C, 2011, 115, 6975-6979.	1.5	15
167	Current rectification induced by V-doped and Sc-doped in Ti2CO2 devices. Computational Materials Science, 2017, 138, 175-182.	1.4	15
168	Nickel-induced transformation of diamond into graphite and carbon nanotubes and the electron field emission properties of resulting composite films. Applied Surface Science, 2018, 428, 264-271.	3.1	15
169	Surfactant-assisted fabrication of graphene frameworks endowing epoxy composites with superior thermal conductivity. Chinese Chemical Letters, 2020, 31, 244-248.	4.8	15
170	Layer-by-layer stacked graphene nanocoatings by Marangoni self-assembly for corrosion protection of stainless steel. Chinese Chemical Letters, 2021, 32, 501-505.	4.8	15
171	Antifouling nanoporous diamond membrane for enhanced detection of dopamine in human serum. Journal of Materials Science, 2021, 56, 746-761.	1.7	15
172	The dimensionality effect on phonon localization in graphene/hexagonal boron nitride superlattices. 2D Materials, 2020, 7, 035029.	2.0	15
173	A Double-Deck Structure of Reduced Graphene Oxide Modified Porous Ti3C2Tx Electrode towards Ultrasensitive and Simultaneous Detection of Dopamine and Uric Acid. Biosensors, 2021, 11, 462.	2.3	15
174	Phase stability, bonding and electrical conduction of amorphous carbon-added Sb films. Scripta Materialia, 2011, 65, 950-953.	2.6	14
175	Optical properties of nitrogen-doped graphene thin films probed by spectroscopic ellipsometry. Thin Solid Films, 2014, 571, 675-679.	0.8	14
176	A study of the growth-time effect on graphene layer number based on a Cu–Ni bilayer catalyst system. RSC Advances, 2016, 6, 23956-23960.	1.7	14
177	Advances in graphene-based polymer composites with high thermal conductivity. Veruscript Functional Nanomaterials, 2018, 2, 1-17.	0.2	14
178	Cone-stacked carbon nanofibers with cone angle increasing along the longitudinal axis. Carbon, 2007, 45, 411-415.	5.4	13
179	Graphene as a nanofiller for enhancing the tribological properties and thermal conductivity of base grease. RSC Advances, 2019, 9, 42481-42488.	1.7	13
180	ZnO nanoflowers modified with RuO2 for enhancing acetone sensing performance. Nanotechnology, 2020, 31, 115502.	1.3	13

#	Article	IF	CITATIONS
181	Theoretical study on the electrical and mechanical properties of MXene multilayer structures through strain regulation. Chemical Physics Letters, 2020, 760, 137997.	1.2	13
182	Analysis of coumarin in food and plant tissue without extraction based on voltammetry of microparticles. Journal of Food Measurement and Characterization, 2021, 15, 5439-5444.	1.6	13
183	Surface modification on copper particles toward graphene reinforced copper matrix composites for electrical engineering application. Journal of Alloys and Compounds, 2022, 891, 162058.	2.8	13
184	Structures and Mechanical Properties of CH <sub>4</sub> , SO <sub>2</sub> , and H <sub>2</sub> S Hydrates from Density Function Theory Calculations. Chemistry Letters, 2017, 46, 1141-1144.	0.7	12
185	Aluminum Borate/Boron Nitride Nanosheet Fibers for Enhancing the Thermal Conductivity of Polymer Composites. ACS Applied Nano Materials, 2021, 4, 2136-2142.	2.4	12
186	Early sex determination of Ginkgo biloba based on the differences in the electrocatalytic performance of extracted peroxidase. Bioelectrochemistry, 2021, 140, 107829.	2.4	12
187	The evolution of mechanical and structural properties at the fiber/matrix interphase of SiC/SiC composites. Computational Materials Science, 2015, 104, 84-91.	1.4	11
188	Superior field emission performance of graphene/carbon nanofilament hybrids synthesized by electrochemical self-exfoliation. Materials Letters, 2017, 205, 223-225.	1.3	11
189	A theoretical investigation and synthesis of layered ternary carbide system U-Al-C. Ceramics International, 2018, 44, 1646-1652.	2.3	11
190	Electrochemical Enantiomer Recognition Based on sp3-to-sp2 Converted Regenerative Graphene/Diamond Electrode. Nanomaterials, 2018, 8, 1050.	1.9	11
191	High-quality graphene transfer <i>via</i> directional etching of metal substrates. Nanoscale, 2019, 11, 16001-16006.	2.8	11
192	Pt nanodendrites with (111) crystalline facet as an efficient, stable and pH-universal catalyst for electrochemical hydrogen production. Chinese Chemical Letters, 2020, 31, 2478-2482.	4.8	11
193	Hydrophilic modification of carbon nanotube to prepare a novel porous copper network-carbon nanotube/erythritol composite phase change material. Composite Interfaces, 2021, 28, 175-189.	1.3	11
194	Construction of Oriented Interconnected BNNS Skeleton by Selfâ€Growing CNTs Leading High Thermal Conductivity. Advanced Materials Interfaces, 2021, 8, 2001910.	1.9	11
195	In-situ synthesis of graphene-like carbon encapsulated copper particles for reinforcing copper matrix composites. Materials and Design, 2021, 203, 109586.	3.3	11
196	A Spiral Graphene Framework Containing Highly Ordered Graphene Microtubes for Polymer Composites with Superior <scp>Throughâ€Plane</scp> Thermal Conductivity. Chinese Journal of Chemistry, 2022, 40, 329-336.	2.6	11
197	First-principles study of magnetism in some novel MXene materials. RSC Advances, 2020, 10, 44430-44436.	1.7	11
198	Structural, electronic and mechanical properties of (NbxTi1â^'x)2SC and (NbxZr1â^'x)2SC (0⩽x⩽1) from first-principles investigations. Computational and Theoretical Chemistry, 2016, 1090, 58-66.	1.1	10

#	Article	IF	CITATIONS
199	Crystal structures and mechanical properties of M (Mg, Sr, Ba, La) x Ca 1â^'x B 6 solid solution: A first principles study. Ceramics International, 2016, 42, 6632-6639.	2.3	10
200	Enhanced thermal transport performance for poly(vinylidene fluoride) composites with superfullerene. Fibers and Polymers, 2017, 18, 1180-1186.	1.1	10
201	A novel porous Mo <sub>3</sub> N <sub>2</sub> /MoO <sub>3</sub> hybrid nanobelt as supercapacitor electrode material. Nano Futures, 2018, 2, 045001.	1.0	10
202	Theoretical exploration on the vibrational and mechanical properties of M <sub>3</sub> C <sub>2</sub> /M <sub>3</sub> C <sub>2</sub> T <sub>2</sub> MXenes. International Journal of Quantum Chemistry, 2020, 120, e26409.	1.0	10
203	Thermal CVD growth of graphene on copper particles targeting tungsten-copper composites with superior wear and arc ablation resistance properties. Diamond and Related Materials, 2020, 104, 107765.	1.8	10
204	Constructing zebra skin structured graphene/copper composites with ultrahigh thermal conductivity. Composites Communications, 2021, 25, 100704.	3.3	10
205	Enzyme-catalyzed deposition of polydopamine for amplifying the signal inhibition to a novel Prussian blue-nanocomposite and ultrasensitive electrochemical immunosensing. Journal of Materials Science and Technology, 2022, 102, 166-173.	5.6	10
206	β-Cyclodextrin-Immobilized Ni/Graphene Electrode for Electrochemical Enantiorecognition of Phenylalanine. Materials, 2020, 13, 777.	1.3	10
207	Enhanced thermal transportation across an electrostatic self-assembly of black phosphorene and boron nitride nanosheets in flexible composite films. Nanoscale, 2022, 14, 9743-9753.	2.8	10
208	Charge dynamics and electronic structures of monolayer graphene with molecular doping. Applied Physics Letters, 2012, 101, 111907.	1.5	9
209	Influence of helium atoms on the shear behavior of the fiber/matrix interphase of SiC/SiC composite. Journal of Nuclear Materials, 2016, 479, 504-514.	1.3	9
210	Field emission properties of the caterpillar-like structural carbon film grown by magnetic and electric fields coupling HFCVD. Applied Surface Science, 2017, 423, 788-792.	3.1	9
211	CVD Synthesis of Monodisperse Graphene/Cu Microparticles with High Corrosion Resistance in Cu Etchant. Materials, 2018, 11, 1459.	1.3	9
212	Cauliflowerâ€like Platinum Particles Decorated Reduced Graphene Oxide for Sensitive Determination of Acetaminophen. Electroanalysis, 2019, 31, 1758-1768.	1.5	9
213	The effect of heat treatment time on the carbon-coated nickel nanoparticles modified boron-doped diamond composite electrode for non-enzymatic glucose sensing. Journal of Electroanalytical Chemistry, 2019, 841, 148-157.	1.9	9
214	High Thermal Conductivity and Anisotropy Values of Aligned Graphite Flakes/Copper Foil Composites. Materials, 2020, 13, 46.	1.3	9
215	The application of molecular simulation in ash chemistry of coal. Chinese Journal of Chemical Engineering, 2020, 28, 2723-2732.	1.7	9
216	Constructing a three-dimensional nano-crystalline diamond network within polymer composites for enhanced thermal conductivity. Nanoscale, 2021, 13, 18657-18664.	2.8	9

#	Article	IF	CITATIONS
217	Effect of magnetic and electric coupling fields on micro- and nano- structure of carbon films in the CVD diamond process and their electron field emission property. Materials Research Express, 2018, 5, 035009.	0.8	7
218	Abnormal grain growth of UO2 with pores in the final stage of sintering: A phase field study. Computational Materials Science, 2018, 145, 24-34.	1.4	7
219	Enzymatic deposition of gold nanoparticles at vertically aligned carbon nanotubes for electrochemical stripping analysis and ultrasensitive immunosensing of carcinoembryonic antigen. Analyst, The, 2020, 145, 3073-3080.	1.7	7
220	Preparation of cassava fiber-iron nanoparticles composite for electrochemical determination of tea polyphenol. Journal of Food Measurement and Characterization, 2021, 15, 4711-4717.	1.6	7
221	Unraveling the strong coupling between graphene/nickel interface and atmospheric adsorbates for versatile realistic applications. Carbon Trends, 2021, 2, 100013.	1.4	7
222	Two-Dimensional Hexagonal Boron Nitride Nanosheets as Lateral Heat Spreader With High Thermal Conductivity. Frontiers in Materials, 2022, 8, .	1.2	7
223	Annealing temperature regulating the dispersity and composition of nickel-carbon nanoparticles for enhanced glucose sensing. Journal of Electroanalytical Chemistry, 2020, 859, 113827.	1.9	6
224	A dense graphene monolith with poloxamer prefunctionalization enabling aqueous redispersion to obtain solubilized graphene sheets. Chinese Chemical Letters, 2020, 31, 2507-2511.	4.8	6
225	Carbon nano-onions as a nanofiller for enhancing thermal conductivity of epoxy composites. Applied Nanoscience (Switzerland), 2023, 13, 483-491.	1.6	6
226	Facile Graphene Transfer Using Commercially Available Liquid Bandage. ACS Applied Nano Materials, 2021, 4, 7272-7279.	2.4	6
227	Universal Principle for Large-Scale Production of a High-Quality Two-Dimensional Monolayer via Positive Charge-Driven Exfoliation. Journal of Physical Chemistry Letters, 2022, 13, 6597-6603.	2.1	6
228	Elucidation of heterogeneous graphene nucleation and growth through Cu surface engineering. Carbon, 2019, 147, 120-125.	5.4	5
229	Voltammetric immunoassay of human IgG based on the release of cadmium(II) from CdS nanocrystals deposited on mesoporous silica nanospheres. Mikrochimica Acta, 2019, 186, 15.	2.5	5
230	Black phosphorene-cellulose nanofiber hybrid paper as flexible heat spreader. 2D Materials, 2021, 8, 045029.	2.0	5
231	Enhanced Thermal Conductivity of Polymer Composite by Adding Fishbone-like Silicon Carbide. Nanomaterials, 2021, 11, 2891.	1.9	5
232	Dually enhanced homogenous synthesis of molybdophosphate by hybridization chain reaction and enzyme nanotags for theÂelectrochemical bioassay of carcinoembryonic antigen. Mikrochimica Acta, 2020, 187, 361.	2.5	4
233	Significant enhancement of corrosion resistance of stainless steel with nanostructured carbon coatings by substrate-catalytic CVD. Applied Nanoscience (Switzerland), 2021, 11, 725-733.	1.6	4
234	Flexible MXene/copper/cellulose nanofiber heat spreader films with enhanced thermal conductivity. Nanotechnology Reviews, 2022, 11, 1583-1591.	2.6	4

#	Article	IF	CITATIONS
235	Quantitative appraisal of the interfacial anchoring state of polyaromatic hydrocarbons during the formation of C/C composites. Carbon, 2010, 48, 1049-1055.	5.4	3
236	Growth of copper on diatom silica by electroless deposition technique. Materials Science-Poland, 2013, 31, 226-231.	0.4	2
237	Strain Sensors: Largeâ€Area Ultrathin Graphene Films by Single‣tep Marangoni Selfâ€Assembly for Highly Sensitive Strain Sensing Application (Adv. Funct. Mater. 9/2016). Advanced Functional Materials, 2016, 26, 1488-1488.	7.8	2
238	Electroanalytical determination of vanillin using PdZn particles decorated ZnS fibers. Journal of Food Measurement and Characterization, 2021, 15, 4718-4725.	1.6	2
239	Natural Graphene Plasmonic <scp>Nanoâ€Resonators</scp> for Highly Active <scp>Surfaceâ€Enhanced</scp> Raman Scattering Platforms. Energy and Environmental Materials, 2023, 6, .	7.3	2
240	Photodetectors: A Broadband Fluorographene Photodetector (Adv. Mater. 22/2017). Advanced Materials, 2017, 29, .	11.1	1
241	Thiolated poly(aspartic acid)-functionalized two-dimensional MoS <sub>2</sub> , chitosan and bismuth film as a sensor platform for cadmium ion detection. RSC Advances, 2020, 10, 37989-37994.	1.7	1
242	Development of a Phase Field Tool Coupling With Thermodynamic Data for Microstructure Evolution Simulation of Alloys in Nuclear Reactors. Frontiers in Materials, 2021, 8, .	1.2	1
243	Environment induced variation in the photoconductivity of graphene observed by terahertz spectroscopy. , 2012, , .		0
244	A parylene micropipette array for enabling simultaneous detection of different target analytes on a CMOS sensor array. , 2016, , .		0
245	Properties of Diamonds and Their Application in Photodetectors. , 2021, , 1871-1896.		0
246	Properties of Diamonds and Their Application in Photodetectors. , 2020, , 1-26.		0